*antioxidants*

MDPI

*Article*

# Loss of ABCC6 in Human Mesenchymal Stem Cells Leads to Elevated Reactive Oxygen Species Formation and a Senescence-like Phenotype

**Michel R. Osterhage [1,2], Cornelius Knabbe [1,2] and Doris Hendig [1,2,*]**

[1] Herz- und Diabeteszentrum Nordrhein-Westfalen, Institut für Laboratoriums- und Transfusionsmedizin, Universitätsklinik der Ruhr-Universität Bochum, 32545 Bad Oeynhausen, Germany
[2] Herz- und Diabeteszentrum Nordrhein-Westfalen, Medizinische Fakultät OWL (Universität Bielefeld), 32545 Bad Oeynhausen, Germany
* Correspondence: dhendig@hdz-nrw.de

**Abstract**

Pseudoxanthoma elasticum (PXE) is an autosomal-recessive disorder caused by mutations in ATP-binding cassette subfamily C member 6 (ABCC6). In addition to the calcification and fragmentation of elastic fibers as the pathomechanistic cause of PXE, systemic and cellular oxidative stress have been reported. Human mesenchymal stem cells (hMSCs) with an *ABCC6* knockdown were chosen to further investigate the oxidative stress associated with ABCC6 deficiency. The cells were treated with hydrogen peroxide to mimic external oxidative stress and the antioxidant Trolox to examine the cells' reaction to decreased oxidative stress. The level of different types of reactive species (RS) like nitric oxide and reactive oxygen species, the senescent phenotype, oxidative damage and mRNA expression of oxidative stress-related genes were evaluated. Knockdown of *ABCC6* was shown to increase RS levels in hMSCs, induce a p53-dependent senescence-like phenotype and increase oxidative damage, while the mRNA expression of oxidative defense genes was elevated. The *ABCC6*-deficient cells exhibited an altered reaction to additional oxidative stress and the incubation with Trolox reversed these changes induced by *ABCC6* knockdown. Our findings provide further evidence linking *ABCC6*-deficiency to oxidative stress and a senescence-like phenotype, while pointing towards antioxidants as part of a potential treatment for PXE.

**Keywords:** pseudoxanthoma elasticum; ABCC6; oxidative stress; senescence; antioxidants; reactive oxygen species

Check for updates

Academic Editor: Ana B Rodríguez Moratinos

Received: 12 January 2026
Revised: 29 January 2026
Accepted: 5 February 2026
Published: 12 February 2026

**Copyright:** © 2026 by the authors. Licensee MDPI, Basel, Switzerland. This article is an open access article distributed under the terms and conditions of the Creative Commons Attribution (CC BY) license.

## 1. Introduction

The fragmentation and calcification of elastic fibers in connective tissues are hallmarks of the autosomal-recessive disorder pseudoxanthoma elasticum (PXE, OMIM 264800). The symptoms of PXE comprise extensive wrinkle formation of the skin, neovascularization and bleeding of the eye's Bruch's membrane and calcification of small and medium-sized arteries. The clinical consequences include impairment or loss of central vision, hypertension and intermittent claudication [1].

The genetic cause of PXE is mutations in the gene encoding the transmembrane protein ATP-binding cassette subfamily C member 6 (ABCC6, NG_007558.3) [2]. This ATP-dependent transporter is mainly localized in the liver and the kidneys and only to a small extent in the clinically involved tissues in PXE [3,4]. The substrate of ABCC6 remains

unknown, leading to the emergence of two hypotheses on the pathobiology of PXE [5]. The metabolic hypothesis assumes that mutations in *ABCC6* result in a lack of transport of the substrate from hepatocytes into the bloodstream leading to ectopic calcification. The cellular hypothesis claims that the loss of functional ABCC6 protein in peripheral cells alters their metabolism and, thus, promotes the calcification of elastic fibers in their proximity [6].

Excessive oxidative stress has been reported in the context of PXE, on both a cellular and systemic level. An increased mitochondrial membrane potential, elevated levels of mitochondrial superoxide and differential mitochondrial protein expression were detected in fibroblasts from PXE patients in comparison to those of healthy donors [7]. Pasquali-Ronchetti et al. were able to detect elevated levels of intracellular superoxide and an increase in hydrogen peroxide production. Furthermore, a decrease in antioxidative capacity and elevated levels of lipid peroxidation, a consequence of oxidative stress, were detected [8]. Garcia-Fernandez et al. detected a lower antioxidative capacity and higher levels of oxidative stress parameters in the circulation of PXE patients [9].

One mechanism of multicellular organisms to prevent the accumulation of DNA damage is called senescence, divided into replicative and acute senescence. Replicative senescence is typically induced by a shortening of the telomers of chromosomes during cell division, activating the DNA damage response and, thus, senescence [10]. Acute senescence is typically induced by stressors such as oxidative stress, oncogenes or ultraviolet radiation, ultimately leading to DNA damage as well [11]. The DNA damage in both types of senescence leads to the stabilization of one or more of the cyclin-dependent kinase inhibitors p53/p21 and p16 [12]. Consequently, cell cycle progression is terminated and further senescence characteristics are acquired. One of the latter is an elevated production of reactive species (RS), such as hydrogen peroxide ($H_2O_2$), superoxide ($^{\cdot}O_2^-$) and nitric oxide (NO), that are needed for the maintenance of senescence [13,14]. But RS can also be beneficial for the cell, since they exhibit signaling functions, [15–17]. As a result, the balance between the formation and degradation of RS is required for normal cellular function. Endogenous antioxidants, such as superoxide dismutase, catalase (CAT), and glutathione, synthesized by the glutathione synthetase (GSS) and glutathione peroxidases (GPX) or exogenous antioxidants, such as vitamin E and C or carotenoids, can be used to counteract excessive RS formation [18]. Sirtuins are a family of histone deacetylases that consist of seven members (SIRT1–7) with different functions in processes associated with oxidative stress defense [19,20]. The activation of SIRT1, for example, leads to reduced lipid peroxidation, measured by the peroxidation product 4-hydroxynonenal (4-HNE) [19]. Tumor necrosis factor receptor associated protein 1 (TRAP1) is a mitochondria-localized member of the heat shock protein family and known to decrease the production of RS [21].

Another important hallmark of senescence is the senescence-associated secretory phenotype, which is characterized by the increased expression and secretion of cytokines, such as interleukin (IL) 1β, IL-6 and IL-8 [22]. Furthermore, most senescent cells exhibit an increased activity of the senescence-associated β-galactosidase, which can act as a marker of the senescent state of the cells [23].

Recent studies in *Abcc6* knockout mice have emphasized a possible role of the bone marrow in PXE pathogenesis [24]. Therefore, bone marrow-derived mesenchymal stem cells were chosen for this investigation. Furthermore, impaired lipid trafficking in adipocytes generated from *ABCC6*-deficient mesenchymal stem cells was detected [25]. The influence of *ABCC6* knockdown on RS levels, senescence and oxidative damage and defense were investigated in this study. Incubation with $H_2O_2$ was chosen to induce acute senescence and mimic systemic oxidative stress, while the antioxidant Trolox was used to diminish RS levels and oxidative stress.

## 2. Materials and Methods

### *2.1. Cell Culture and Treatment*

Human bone marrow-derived mesenchymal stem cells (hMSCs, see Table 1) were purchased from PromoCell (Heidelberg, Germany) and cultivated in a mesenchymal stem cell growth medium kit (MSCGM, Lonza, Basel, Switzerland) according to the manufacturer's instructions. The cells were sub-cultured upon reaching approximately 90% confluence. Cells in passage 10 were used for experiments.

**Table 1.** Denotation and characteristics of the hMSCs used in this study.

| Denotation | Sex | Age | Lot |
|---|---|---|---|
| hMSC-f | Female | 66 | 451Z012.3 |
| hMSC-m | Male | 68 | 467Z023.5 |

The hMSCs were seeded at a density of 4000 cells/cm$^2$ in MSCGM for the induction of acute senescence and implementation of additional oxidative stress. The cells were treated 24 h later with 2 mM Trolox (1 mM $Na_2CO_3$, Merck, Darmstadt, Germany) with or without 1 mM $H_2O_2$ (Roth, Karlsruhe, Germany) or with 1 mM $Na_2CO_3$ (vehicle) in MSCGM with delipidated FCS (dFCS). After incubation with $H_2O_2$, cells were washed with 1× DPBS, given fresh dFCS MSCGM with or without Trolox and cultivated for an additional 72 h. Trolox concentration was selected by testing different concentrations using a WST1-cell proliferation assay. Control cells were cultivated in dFCS MSCGM without $H_2O_2$ following the same schedule.

### *2.2. Delipidation of FCS*

The delipidation of FCS was performed by the incubation of 50 mL FCS (MCGS, Lonza, Basel, Switzerland) with 1 g of Cab-o-sil (Sigma-Aldrich, St. Louis, MO, USA) overnight at 4 °C. The mixture was then centrifugated at 4 °C and 10,000× *g* for 1 h and the delipidated FCS from the supernatant was sterile filtered using a 0.22 µm filter.

### *2.3. ABCC6 Knockdown via CRISPR/Cas9*

The transfection of a ribonucleoprotein complex for CRISPR/Cas9-mediated ABCC6 knockdown was performed in accordance with Plümers et al. and the transfection protocol from IDT (Coralville, IA, USA) [25].

### *2.4. Nucleic Acid Isolation*

The isolation of genomic DNA was performed using the NucleoSpin Blood Kit (Macherey-Nagel, Düren, Germany), following the manufacturer's instructions. RNA was isolated using the NucleoSpin RNA Kit (Macherey-Nagel, Düren, Germany), according to the manufacturer's instructions. The concentration of DNA and RNA was measured using the NanoDrop2000 spectrophotometer (Peqlab, Erlangen, Germany).

### *2.5. Assessment of Reactive Oxygen and Nitrogen Species*

The levels of reactive oxygen and nitrogen species were measured using different fluorescent probes. The hMSCs were seeded and treated according to Section 2.1. After 72 h of incubation, the cells were stained with different concentrations of the fluorescent probes for different time periods (see Table 2). Cells were stained using the Viobility™ 640/770 Fixable Dye (Miltenyi Biotec, Bergisch Gladbach, Germany) 15 min before the RS staining was completed. The cells were washed with 1× DPBS and detached using 1× Trypsin (PAN Biotech, Aidenbach, Germany). After centrifugation for 5 min at 310× *g*, the cells were

resuspended in 1× DPBS and the fluorescence was measured using the BD FACSCanto™ II Flow Cytometer (BD Biosciences, Franklin Lakes, NJ, USA). The fluorescence measurement was performed using biological triplicates and background fluorescence was subtracted using unstained hMSCs. Recorded events were gated for intact cells, singlets and viable cells using the Kaluza Software (Kaluza Analysis 2.3., Beckman Coulter, Brea, CA, USA) and the mean intensity of the events recorded was determined.

**Table 2.** Different fluorescent probes.

| Fluorescent Probe | Abbreviation | Working Concentration [µM] | Incubation Time [min] |
|---|---|---|---|
| Carboxy-H2DCFDA (6-Carboxy-2′,7′-Dichlordihydrofluorescein-Diacetat) | DCFDA | 10 | 60 |
| DAF-FM Diacetate (4-Amino-5-Methylamino-2′,7′-Difluorofluorescein Diacetate) | DAF-FM | 10 | 60 |

### *2.6. Immunofluorescence Staining and Fluorescence Microscopy*

After the cell treatment, cells were seeded on 8-well µ-slides (ibidi, Gräfelfing, Germany) at a density of 4000 cells/cm$^2$ and cultivated for an additional 24 h. The medium was removed, and the cells were washed with 1× DPBS and fixated using 4% paraformaldehyde (Roth, Karlsruhe, Germany) for 15 min. Permeabilization was performed using 0.1% Triton-X-100 (Roth, Karlsruhe, Germany) in 1× DPBS for 10 min and unspecific binding sites were blocked using 5% normal goat serum (Cell Signaling Technology, Cambridge, United Kingdom) in 1× DPBS for 1 h. Primary antibodies were diluted in 5% normal goat serum according to Table 3 and incubated on the cells for 2 h.

**Table 3.** Primary antibodies used in this study. Target protein, host species, dilution and manufacturer are included.

| Target | Host Species | Dilution | Manufacturer |
|---|---|---|---|
| p21 | Rabbit | 1:200 | ab109520 Abcam, Cambridge, MA, USA |
| p53 | Mouse | 1:400 | sc-126 Santa Cruz, Dallas, TX, USA |
| 4-HNE | Mouse | 1:50 | XG3647431 Invitrogen, Carlsbad, CA, USA |

Species-specific fluorescence-conjugated secondary antibodies were diluted in 5% normal goat serum and incubated with the cells for 1 h before staining the nuclei using 5 µg/mL Hoechst (Abcam, Cambridge, MA, USA). Cells were mounted with ROTI®Mount FluorCare mounting media (Roth, Karlsruhe, Germany) and images were captured using the BZ-X810 microscope (Keyence, Osaka, Japan). The image processing and determination of fluorescence intensity was performed using ImageJ 1.52a (National Institutes of Health, Bethesda, MD, USA). For quantification of fluorescence intensity, images were converted to greyscale and identical acquisition settings were used for all compared conditions. Regions of interest were defined manually and mean fluorescence intensity was measured.

### *2.7. β-Galactosidase Assay*

The β-galactosidase activity was measured using a fluorescence-based assay [26]. The hMSCs were treated as described in 4.1 and incubated for 72 h. Lysis of the cells was

performed using 300 µL lysis buffer (pH 6.0, see Table 4) and the lysate was frozen at −80 °C until the assay was performed. The lysate was centrifuged at 12,000× *g* and 4 °C for 5 min. An amount of 100 µL of the supernatant was mixed with 100 µL of 2× reaction buffer (see Table 5) and incubated for 1 h at 37 °C.

**Table 4.** Composition of the lysis buffer used for the β-galactosidase assay. Benzamidine and PMSF were added right before performing lysis.

| Component | Concentration [mM] |
|---|---|
| 3-[(3-Cholamidopropyl)dimethylammonio]-1-propanesulfonate (CHAPS) | 5 |
| Citric acid | 40 |
| Sodium phosphate | 40 |
| Benzamidine | 0.5 |
| Phenylmethanesulfonyl fluoride (PMSF) | 0.25 |
| Water | ad. 15 mL |

**Table 5.** Composition of the 2× reaction buffer used for the β-galactosidase assay. The fluorogenic substrate MUG was dissolved in dimethyl sulfoxide (DMSO) at a concentration of 34 mM.

| Component | Concentration/mM |
|---|---|
| Citric acid | 40 |
| Sodium phosphate | 40 |
| Sodium chloride | 300 |
| β-mercaptoethanol | 10 |
| Magnesium chloride | 4 |
| 4-methylumbelliferyl-β-D-galactopyranoside (MUG) | 1.7 |
| Water | *ad*. 50 mL |

The reaction was stopped using 600 µL of a 400 mM sodium carbonate solution and the fluorescence was measured on the Tecan Reader Infinite 200 Pro (Tecan, Männedorf, Switzerland). The fluorescence intensity detected was normalized to the protein concentration determined using a bicichonic acid assay (Merck, Darmstadt, Germany).

### *2.8. Gene Expression Analysis*

An amount of 1 µg of isolated RNA was transcribed to complementary DNA using the GoScript™ Reverse Transcriptase Kit (Promega, Madison, WI, USA) following the manufacturer's instructions. Quantitative real-time polymerase chain reaction (qRT-PCR) was performed using 5 µL LightCycler 480 SYBR Green I Master reaction mixture (Roche, Basel, Switzerland), 0.25 µL each of 25 µM forward and reverse primers (Biomers, Ulm, Germany), 2 µL water and 2.5 µL 1:10 diluted complementary DNA in a 384-well plate (Sarstedt, Nümbrecht, Germany). The PCR reaction consisted of an initial denaturation at 95 °C for 5 min, followed by 45 cycles of amplification including denaturation at 95 °C for 10 s, annealing at a primer-specific temperature (Table 6) for 15 s and elongation at 72 °C for 20 s.

The Ct values detected of genes of interest were normalized to the mean of expression of the three housekeeping genes *ribosomal protein L13a* (*RPL13A*), *succinate dehydrogenase complex flavoprotein subunit A* (*SDHA*) and *beta-2-microglobulin* (*β2M*) using the efficiency-corrected delta-delta Ct method.

**Table 6.** Primers used for qRT-PCR in this study.

| Gene | 5′-3′ Sequence | Annealing Temperature | Efficiency |
|---|---|---|---|
| *CAT* | AAACCGCACGCTATGGCTGA<br>AAAGTAGCCAAAGGCCCCTGC | 63 | 1.99 |
| *GPX1* | TGGCCTCCCCTTACAGTGCT<br>TCTTGGCGTTCTCCTGATGCC | 66 | 2.00 |
| *GPX4* | TCCCAGTGAGGCAAGACCGA<br>AGAGACGGTGTCCAAACTTGGTG | 66 | 2.00 |
| *GSS* | TCGCGGAGGAAAGGCGAAC<br>GCGATTCAGGCCCAGGAACA | 63 | 1.90 |
| *p21* | GCAGACCAGCATGACAGATTTC<br>ACCTCCGGGAGAGAGGAAAA | 66 | 1.81 |
| *p53* | AGATAGCGATGGTCTGGC<br>TTGGGCAGTGCTCGCTTAGT | 63 | 2.00 |
| *RPL13A* | CGGAAGGTGGTGGTCGTA<br>CTCGGGAAGGGTTGGTGT | 63 | 1.87 |
| *SDHA* | AACTCGCTCTTGGACCTG<br>GAGTCGCAGTTCCGATGT | 63 | 1.93 |
| *SIRT2* | ATCCCCGACTTTCGCTCTC<br>GGTTGGCTTGAACTGCCCA | 66 | 1.86 |
| *SIRT3* | CCTCTGCCACCTGCACAGTC<br>TGGGGGCAGCCATCATCCTA | 63 | 1.93 |
| *SIRT6* | TGCGAGCCTGCAGGGGAGA<br>CAGCGATGTACCCAGCGTGATG | 63 | 1.77 |
| *SIRT7* | GGTCGTCTACACAGGCGCGG<br>TCCCTGTTGGGAACGCAGGA | 63 | 1.86 |
| *TRAP1* | GTGCCGGGAGGAAAACCAA<br>TGTTTGGAAGTGGAACCCTGC | 66 | 2.00 |
| *β2M* | TGTGCTCGCGCTACTCTCTCTT<br>CGGATGGATGAAACCCAGACA | 63 | 1.85 |

### *2.9. Statistical Analysis*

Statistical analysis was performed using the GraphPad Prism 10 software (GraphPad, San Diego, CA, USA). All experiments were performed in biological and technical triplicates. The data shown are presented as mean values ± standard error of mean and statistical significance was calculated using three-way ANOVA and Tukey's multiple comparisons test with probability ($p$) values equal or below 0.05 being considered statistically significant.

## 3. Results

### *3.1. Elevated Levels of Reactive Species May Be the Cause of the Senescence-like Phenotype*

Based on our previous work, a CRISPR/Cas9-based approach for *ABCC6* knockdown was chosen [26]. This gene editing model was chosen to achieve a stable reduction in *ABCC6* mRNA expression over several passages. An efficiency of the knockdown of above 70% was determined using the T7 endonuclease I assay, TA-cloning and qRT-PCR (Figures S1–S3).

Evaluation of the effect of *ABCC6*-knockdown on reactive species levels was performed by detecting different fluorescent probes using flow cytometry (Figure S4).

Total reactive oxygen species (ROS) was detected as 4.3-fold (±0.5) higher in $H_2O_2$-treated control cells compared to the untreated cells. The additional incubation with Trolox

resulted in a 63% (±10%) decreased ROS level compared to $H_2O_2$-treated control cells. The knockdown of *ABCC6* led to a 2.9-fold (±0.3) increase in the level of total ROS compared to untreated control cells and the incubation of knockdown cells with Trolox led to an 80% (±4%) reduction in the total ROS level compared to untreated knockdown cells. Hydrogen peroxide elevated the total ROS level 1.8-fold (±0.2) in relation to untreated knockdown cells, while the additional treatment with Trolox led to a 65% (±10%) decrease in the ROS level (Figure 1A).

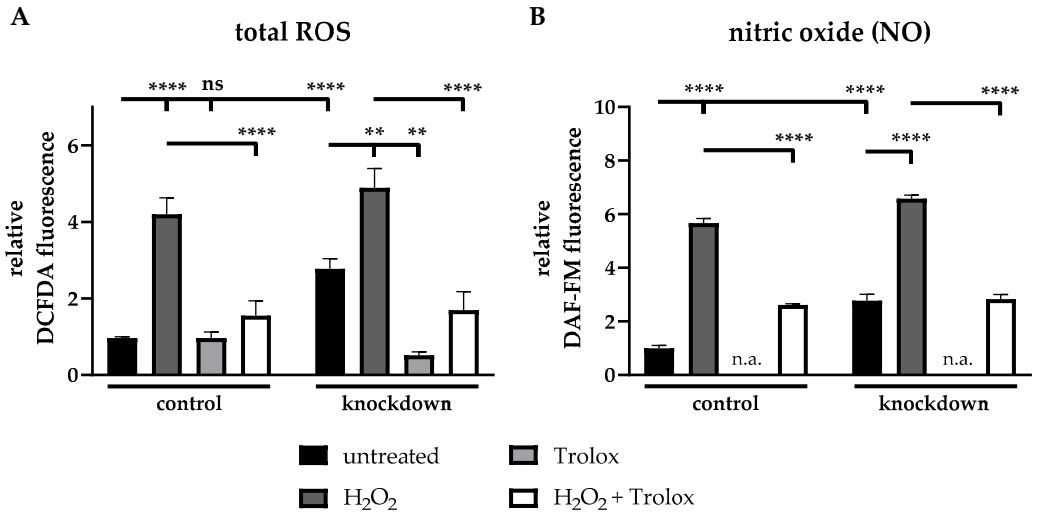



**Figure 1.** Measurement of different types of reactive species in control and knockdown human mesenchymal stem cells (hMSCs). Control and knockdown hMSCs (n = 2) were treated with $H_2O_2$, the antioxidant Trolox, $H_2O_2$ in addition to Trolox or were left untreated for 72 h. Cells were stained using (**A**) 10 µM DCFDA for 1 h and (**B**) 10 µM DAF-FM for 1 h. Additionally, a viability stain was used to label dead cells. After incubation, cells were washed, detached and fluorescence was detected using flow cytometry. Data are shown as mean ± SEM. Statistical significance was determined using three-way ANOVA. ** $p \leq 0.01$, **** $p \leq 0.0001$, ns: not significant.

The incubation of control cells with $H_2O_2$ elevated the nitric oxide (NO) level 5.7-fold (±0.6) compared to untreated cells, while the combined treatment of $H_2O_2$ and Trolox decreased the NO level to 54% (±2%) in relation to $H_2O_2$-treated cells. Due to the knockdown of *ABCC6*, a 2.8-fold (±0.4) higher DAF-FM fluorescence compared to control cells was detected. The incubation with $H_2O_2$ led to a 2.4-fold (±0.2) increase in the fluorescence intensity in knockdown cells compared to untreated knockdown cells and following treatment with $H_2O_2$ and Trolox, a 57% (±3%) decrease in the relative fluorescence intensity was detected compared to $H_2O_2$-treated knockdown cells. The incubation of control and knockdown cells with Trolox reduced the fluorescence intensity to the level of the internal unstained control, consequently, no measurable results were obtained (Figure 1B).

### *3.2. ABCC6 Knockdown hMSCs Reveal a Senescence-like Phenotype*

A potential senescence-like phenotype in knockdown hMSCs was evaluated by measuring the senescence-associated β-galactosidase activity and the mRNA expression of the cell cycle inhibitors *p21* and *p53*.

The incubation of control cells with $H_2O_2$ resulted in a 1.3-fold (±0.1) increase in the relative β-galactosidase activity compared to untreated control cells. The treatment of control cells with Trolox decreased the relative β-galactosidase activity by 30% (±2%) in relation to untreated control cells and the additional treatment of $H_2O_2$ incubated cells with Trolox reduced the β-galactosidase activity by 37% (±3%) compared to $H_2O_2$-treated cells. Due to the knockdown of *ABCC6*, a 1.3-fold (±0.1) increase in the β-galactosidase activity

compared to control cells was detectable. In contrast to control cells, a treatment with $H_2O_2$ resulted in no significantly altered β-galactosidase activity in knockdown cells in comparison to untreated knockdown cells. Treating the knockdown cells with Trolox caused a 40% (±4%) reduction in the relative β-galactosidase activity compared to untreated cells. The combined treatment with $H_2O_2$ and Trolox resulted in a 26% (±6%) decreased activity relative to $H_2O_2$-treated knockdown cells (Figure 2A).

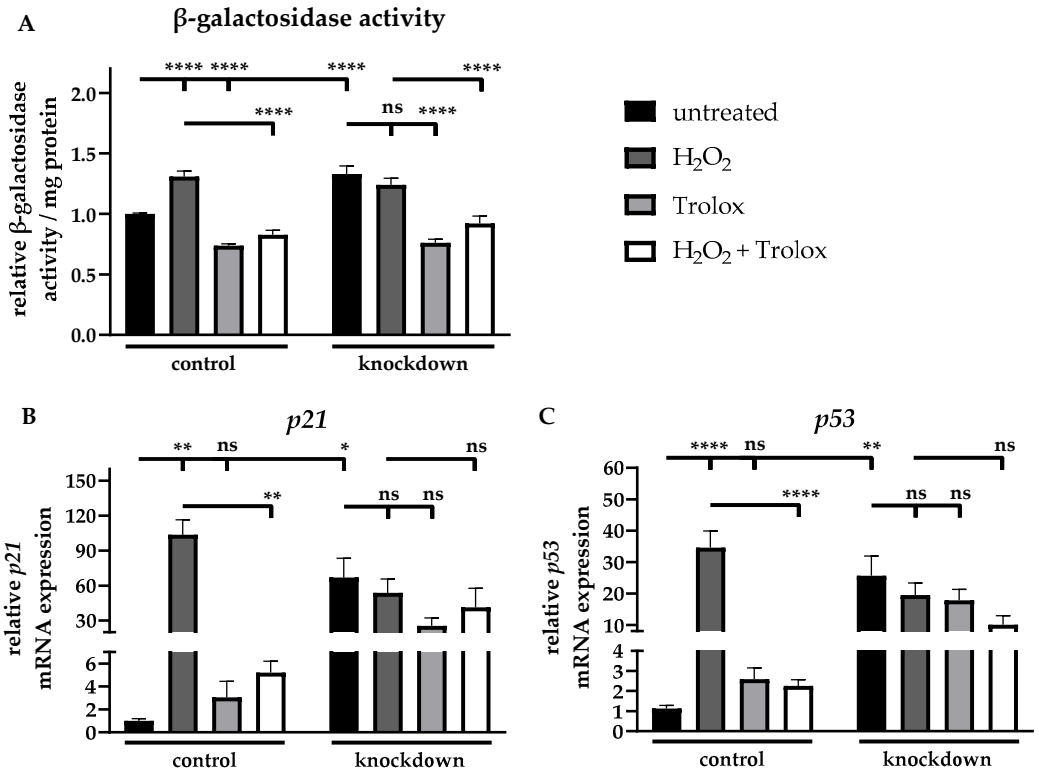



**Figure 2.** Evaluation of the senescent phenotype of *ABCC6* knockdown and control hMSCs. Control and knockdown hMSCs (n = 2) were treated with $H_2O_2$, the antioxidant Trolox, $H_2O_2$ in addition to Trolox or were left untreated for 72 h. (**A**) Cells were lysed and the β-galactosidase activity was measured using a fluorescence assay. The mRNA expression of the cell cycle inhibitors (**B**) *p21* and (**C**) *p53* was detected via qRT-PCR. Data are shown as mean ± SEM. Statistical significance was determined using three-way ANOVA. * $p \leq 0.05$, ** $p \leq 0.01$, **** $p \leq 0.0001$, ns not significant.

Due to the incubation of control cells with $H_2O_2$, a 104-fold (±25.2) increase in *p21* mRNA expression was detected compared to untreated control cells, while the additional treatment with Trolox led to a 95% (±1%) decrease in mRNA expression in relation to $H_2O_2$-treated cells. The cultivation of control cells with Trolox alone did not alter the *p21* mRNA expression compared to untreated cells. The knockdown of *ABCC6* resulted in a 67.2-fold (±21.6) increase in *p21* mRNA expression relative to untreated control cells, while none of the treatments tested had a significant effect on the *p21* mRNA expression of the knockdown cells (Figure 2B).

After the incubation of control cells with $H_2O_2$, the *p53* mRNA expression was detected as 30.4-fold (±6.1) increased compared to untreated control cells, whereas the additional treatment with Trolox resulted a 93% (±1%) decrease in the *p53* mRNA expression in relation to $H_2O_2$-treated cells. The treatment of control cells with Trolox did not lead to any significant changes in the mRNA expression due to the knockdown of *ABCC6*; a 22.6-fold (±6.2) elevated *p53* mRNA expression was measured compared to control cells. None of the treatments performed resulted in an altered *p53* mRNA expression of the knockdown cells compared to the untreated knockdown cells (Figure 2C).

The senescent phenotype was further investigated by immunofluorescent staining of the cell cycle inhibitors p21 and p53, to validate the transcriptional data on the protein level. Using the nucleic counterstain, the area of the nucleus was marked and the fluorescence intensity of the stained cell cycle inhibitors was quantified exclusively in that area.

Following the treatment of control cells with $H_2O_2$, a 1.1-fold (±0.01) increase in relative fluorescence intensity compared to untreated cells was detected. Additional treatment with Trolox resulted in a 1.2-fold (±0.02) increase compared to the $H_2O_2$-treated control cells. Incubation with Trolox resulted in a 1.1-fold (±0.03) elevated fluorescence intensity compared to untreated cells. The knockdown of *ABCC6* resulted in a 20% (±2%) reduction in the fluorescence intensity compared to control cells. The $H_2O_2$-treated cells exhibited a 1.5-fold (±0.03) increase in fluorescence intensity relative to untreated knockdown cells, while the additional treatment with Trolox resulted in a 1.1-fold (±0.02) elevated fluorescence intensity compared to $H_2O_2$-treated cells. Incubation of the knockdown cells with Trolox showed a 1.2-fold (±0.02) elevated relative fluorescence intensity (Figure 3A).

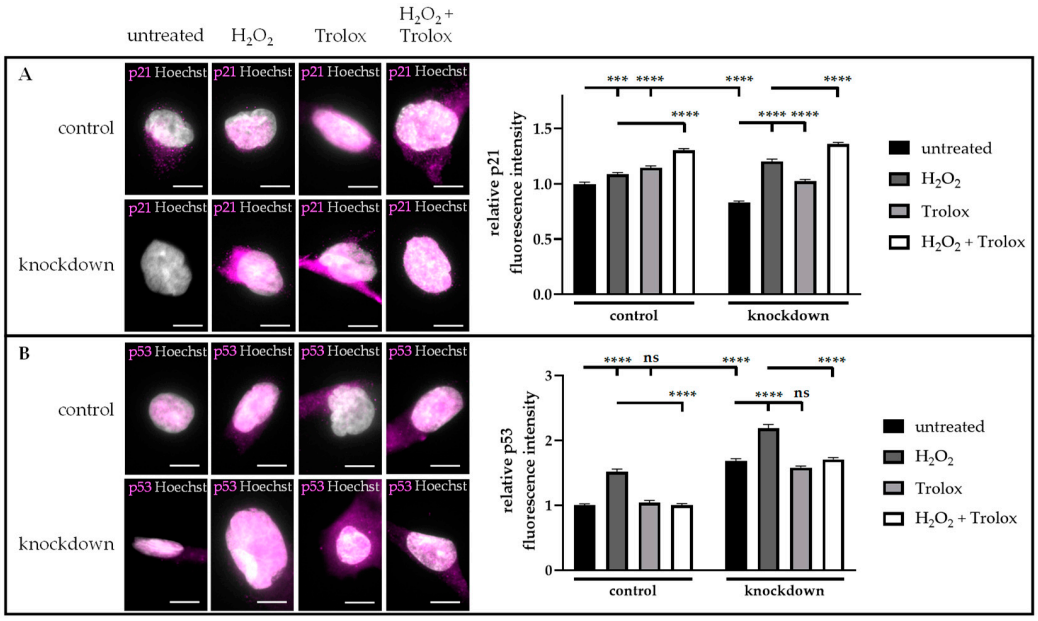



**Figure 3.** Immunofluorescence images and quantification of cell cycle inhibitors. Control and knockdown hMSCs (n = 2) were treated with $H_2O_2$, the antioxidant Trolox, $H_2O_2$ in addition to Trolox or were left untreated for 72 h. Cells were reseeded for immunofluorescence and the cell cycle inhibitors (**A**) p21 and (**B**) p53 (magenta) were stained using specific antibodies. Nuclei were counterstained using Hoechst (grey). Representative images, scale bar 10 µm. Fluorescence intensity in the nucleic area was quantified via ImageJ. Data are shown as mean ± SEM. Statistical significance was determined using three-way ANOVA. *** $p \leq 0.001$, **** $p \leq 0.0001$, ns not significant.

The cultivation of control cells with $H_2O_2$ increased the fluorescence intensity of p53 1.5-fold (±0.05) compared to untreated cells, while the additional treatment with Trolox resulted in a 34% (±2%) reduction in the fluorescence intensity compared to $H_2O_2$-treated control cells. The incubation of control cells with Trolox did not result in any significant changes in the fluorescence intensity in relation to untreated cells. Following the *ABCC6* knockdown, an increase in the fluorescence intensity of 1.7-fold (±0.05) relative to untreated control cells was detected. The treatment of knockdown cells with $H_2O_2$ resulted in a 1.3-fold (±0.04) elevation of the p53 fluorescence intensity compared to untreated knockdown cells. The additional incubation with Trolox led to a 22% (±2%) decrease in the fluorescence intensity compared to $H_2O_2$-treated knockdown cells. The treatment of

knockdown cells with Trolox did not induce any changes in the p53 fluorescence intensity in knockdown cells (Figure 3B).

### *3.3. Knockdown hMSCs Exhibit Differential Patterns of Oxidative Stress*

An assessment of the oxidative damage was performed using immunofluorescence staining of the lipid peroxidation product 4-hydroxynonenal (4-HNE) (Figure 4A).

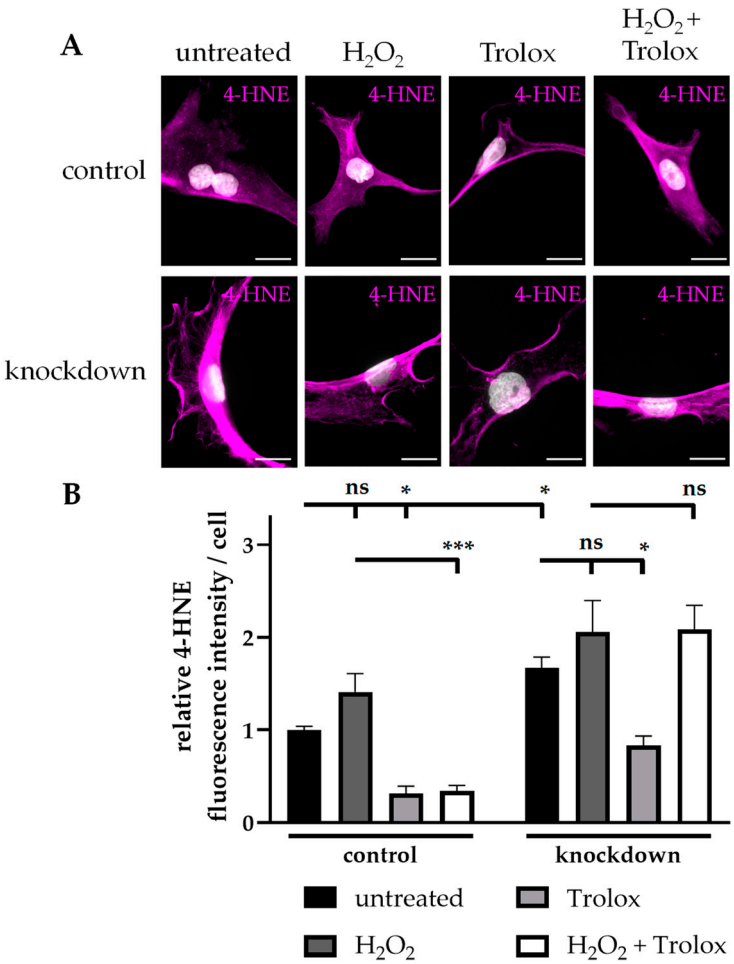



**Figure 4.** Immunofluorescence images and quantification of lipid peroxidation marker 4-HNE. Control and knockdown hMSCs (n = 2) were treated with $H_2O_2$, the antioxidant Trolox, $H_2O_2$ in addition to Trolox or were left untreated for 72 h. (**A**) Cells were reseeded for immunofluorescence and the lipid peroxidation marker 4-HNE (magenta) was stained using a specific antibody. Nuclei were counterstained using Hoechst (grey). Representative images, scale bar 10 µm. (**B**) Fluorescence intensity per cell was measured via ImageJ. Data are shown as mean ± SEM. Statistical significance was determined using three-way ANOVA. * $p \leq 0.05$, *** $p \leq 0.001$, ns: not significant.

The incubation of control cells with $H_2O_2$ did not reveal any significant changes in the 4-HNE fluorescence intensity compared to the untreated control. The treatment of control cells with Trolox led to a 69% (±8%) decrease in the fluorescence intensity relative to untreated cells, while the incubation of $H_2O_2$-treated cells with Trolox resulted in a 66% (±8%) decrease in the fluorescence intensity compared to control cells. Following the knockdown of *ABCC6*, a 1.7-fold (±0.1) increase in the 4-HNE fluorescence intensity was detected. The treatment of knockdown cells with $H_2O_2$ did not alter the fluorescence intensity measured compared to untreated knockdown cells, while the additional incubation with Trolox did not result in any changes either compared to $H_2O_2$-treated cells. The

treatment of knockdown cells with Trolox led to a 50% (±7%) decrease in the fluorescence intensity detected relative to untreated knockdown cells (Figure 4B).

The influence of the *ABCC6* knockdown on the mRNA expression of different genes associated with oxidative stress defense, reactive species (RS) production and RS elimination was investigated using qRT-PCR.

Firstly, the mRNA expression of genes of the sirtuin (SIRT) family was evaluated. Following the $H_2O_2$ treatment, the *SIRT2* mRNA expression of control cells was 17.9-fold (±2.9) increased compared to untreated control cells, while the additional treatment with Trolox resulted in a 93% (±1%) reduction in mRNA expression compared to $H_2O_2$-treated cells. The incubation of control cells with Trolox did not alter the mRNA expression in relation to untreated cells. The ABCC6 deficiency resulted in a 13.4-fold (±2.0) elevated *SIRT2* mRNA expression relative to untreated control cells, while none of the conditions tested altered the mRNA expression in knockdown cells (Figure 5A).

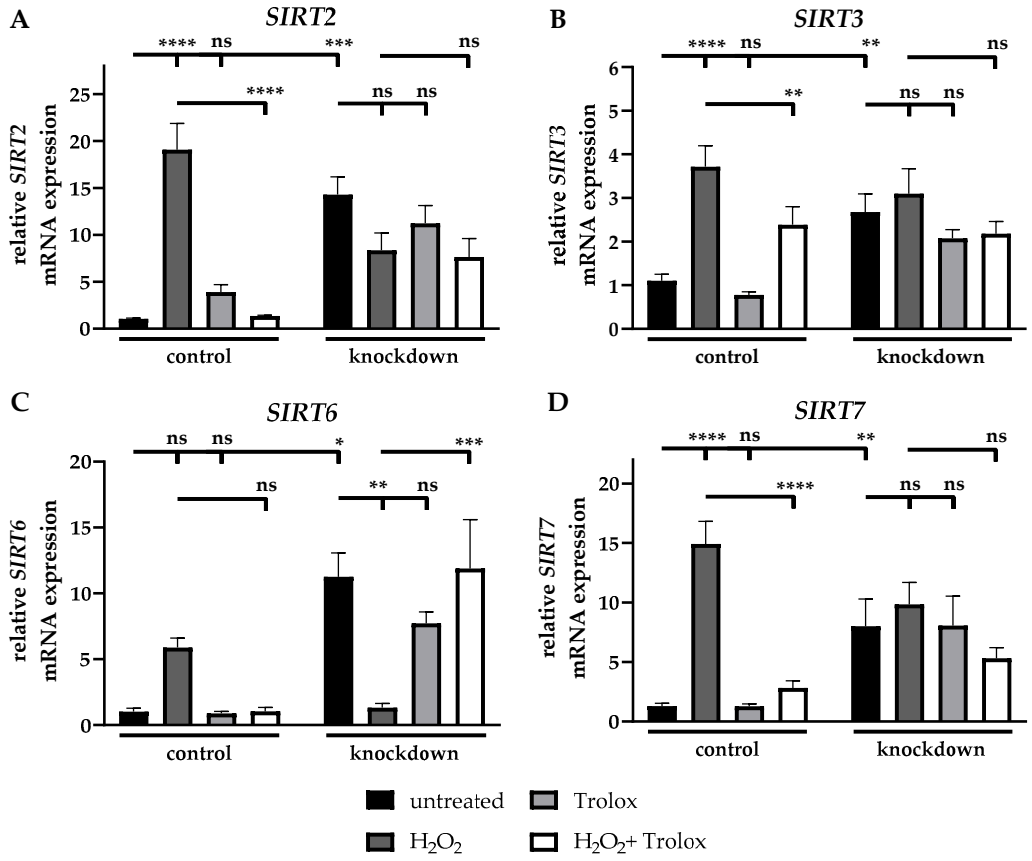



**Figure 5.** The mRNA expression of sirtuins, a family of antioxidative proteins. Control and knockdown hMSCs (n = 2) were treated with $H_2O_2$, the antioxidant Trolox, $H_2O_2$ in addition to Trolox or were left untreated for 72 h. Cells were lysed and qRT-PCR was used to measure the mRNA expression of (**A**) *SIRT2*, (**B**) *SIRT3*, (**C**) *SIRT6* and (**D**) *SIRT7*. Data are shown as mean ± SEM. Statistical significance was determined using three-way ANOVA. * $p \leq 0.05$, ** $p \leq 0.01$, *** $p \leq 0.001$, **** $p \leq 0.0001$, ns not significant.

Regarding the *SIRT3* mRNA expression, the incubation of control cells with $H_2O_2$ resulted in a 3.4-fold (±0.6) increased expression. Additional treatment with Trolox resulted in a 36% (±14%) reduction in mRNA expression compared to $H_2O_2$-treated cells, while the knockdown of *ABCC6* led to a 2.4-fold (±0.5) increase compared to untreated control cells. The other conditions tested did not show any changes in mRNA expression (Figure 5B).

The *SIRT6* mRNA expression was not significantly altered in control cells after treatment with $H_2O_2$, Trolox or their combination. Due to the knockdown of *ABCC6*, a 22.3-fold

(±7.8) elevation in *SIRT6* mRNA expression compared to untreated control cells, was observed. The treatment of knockdown cells with $H_2O_2$ led to a 95% (±1%) reduction in *SIRT6* mRNA expression compared to untreated knockdown cells, while the additional incubation with Trolox led to an 8.9-fold (±3.5) elevated *SIRT6* mRNA expression compared to $H_2O_2$-treated knockdown cells (Figure 5C).

Following the $H_2O_2$ treatment, the mRNA expression of *SIRT7* was detected as 11.5-fold (±2.5) increased relative to the untreated control. The additional incubation with Trolox resulted in an 81% (±5%) reduction compared to $H_2O_2$-treated control cells, while Trolox alone did not alter the mRNA expression in relation to untreated control cells. The knockdown of *ABCC6* led to a 6.1-fold (±2.1) elevated *SIRT7* mRNA expression compared to untreated control cells. None of the conditions tested resulted in changes in the *SIRT7* mRNA expression in knockdown cells compared to untreated knockdown cells (Figure 5D).

The mRNA expression of *glutathione synthetase* (*GSS*) was detected as 6.9-fold (±2.3) increased due to the incubation of control cells with $H_2O_2$ compared to the untreated cells, while the additional incubation with Trolox led to a 71% (±4%) reduction in relation to $H_2O_2$-treated cells. The treatment of control cells with Trolox did not result in any changes in mRNA expression relative to the untreated control. Following the knockdown of *ABCC6*, the mRNA expression of *GSS* was detected as 4.3-fold (±1.4) elevated compared to control cells. None of the treatments performed led to an altered *GSS* mRNA expression in knockdown cells relative to untreated knockdown cells (Figure 6A).

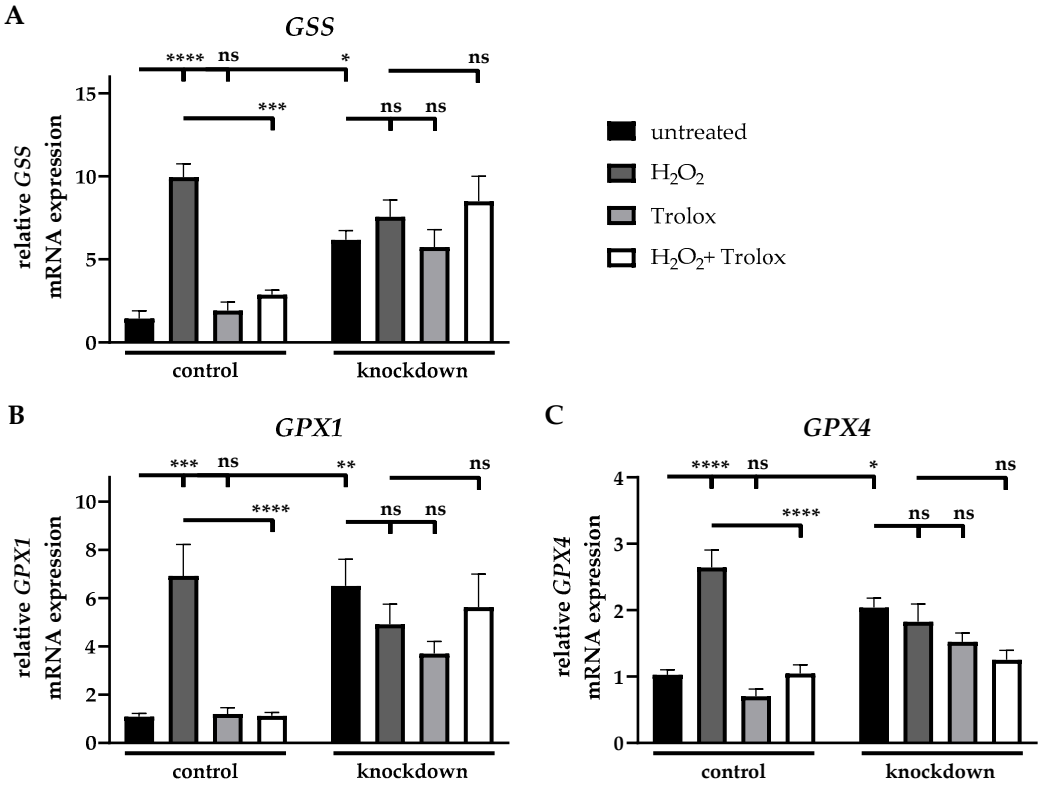



**Figure 6.** The mRNA expression of glutathione-oxidative defense genes. Control and knockdown hMSCs (n = 2) were treated with $H_2O_2$, the antioxidant Trolox, $H_2O_2$ in addition to Trolox or were left untreated for 72 h. Cells were lysed and qRT-PCR was used to measure the mRNA expression of (**A**) *GSS*, (**B**) *GPX1* and (**C**) *GPX4*. Data are shown as mean ± SEM. Statistical significance was determined using three-way ANOVA. * $p \leq 0.05$, ** $p \leq 0.01$, *** $p \leq 0.001$, **** $p \leq 0.0001$, ns: not significant.

After the incubation of control cells with $H_2O_2$, the mRNA expression of *glutathione peroxidase 1* (*GPX1*) was detected as 6.4-fold (±1.4) increased compared to the untreated control. The additional treatment with Trolox led to an 84% (±4%) reduction in relation to $H_2O_2$-treated cells. The incubation of control cells with Trolox did not result in any changes in mRNA expression compared to control cells. The mRNA expression of *GPX1* was measured as 6.0-fold (±1.3) elevated in knockdown cells compared to control cells, while none of the treatments performed was shown to have an effect on *GPX1* mRNA expression in knockdown cells (Figure 6B).

A 2.6-fold (±0.3) increase in the mRNA expression of *GPX4* was detected in control cells following the $H_2O_2$-treatment relative to the untreated control, while the additional treatment with Trolox reduced the mRNA expression to 60% (±6%) relative to $H_2O_2$-treated cells. The knockdown of ABCC6 led to a 2.0-fold (±0.2) elevated mRNA expression of *GPX4* compared to control cells. No alterations in *GPX4* mRNA expression were present compared to the respective control for the other conditions tested (Figure 6C).

The incubation of control cells with $H_2O_2$ induced a 2.1-fold (±0.3) increase in the mRNA expression of *catalase* (*CAT*) compared to untreated control cells, while the additional Trolox treatment reduced the expression to 73% (±4%) relative to $H_2O_2$-treated cells. The incubation of control cells with Trolox alone led to a 60% (±9%) reduction in mRNA expression. Neither the knockdown of *ABCC6*, nor the additional treatments resulted in any alterations in mRNA expression (Figure 7A).

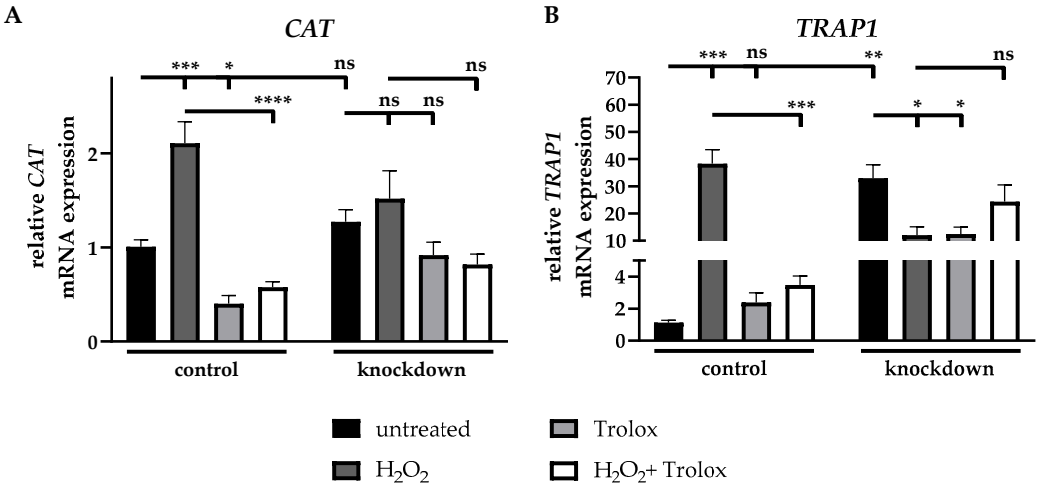



**Figure 7.** The mRNA expression of oxidative stress-related genes. Control and knockdown hMSCs (n = 2) were treated with $H_2O_2$, the antioxidant Trolox, $H_2O_2$ in addition to Trolox or were left untreated for 72 h. Cells were lysed and qRT-PCR was used to measure the mRNA expression of (**A**) *CAT* and (**B**) *TRAP1*. Data are shown as mean ± SEM. Statistical significance was determined using three-way ANOVA. * $p \leq 0.05$, ** $p \leq 0.01$, *** $p \leq 0.001$, **** $p \leq 0.0001$, ns: not significant.

The treatment with $H_2O_2$ led to a 34.1-fold (±6.5) increase in TNF receptor associated protein 1 (*TRAP1*) mRNA expression in control cells relative to untreated cells. Trolox alone did not induce any changes in *TRAP1* mRNA expression, while the treatment with $H_2O_2$ and Trolox resulted in a 91% (±2%) reduction in mRNA expression compared to $H_2O_2$-treated cells. Due to the knockdown of *ABCC6*, a 29.4-fold (±5.9) elevation in mRNA expression compared to control cells was detected. The treatment of knockdown cells with $H_2O_2$ or Trolox resulted in 63% (±11%) and 62% (±10%) decreased *TRAP1* mRNA expression, relatively, compared to untreated knockdown cells, while the combination of $H_2O_2$ and Trolox left the mRNA expression in knockdown cells unchanged in relation to $H_2O_2$-treated cells (Figure 7B).

## 4. Discussion

Pseudoxanthoma elasticum (PXE) is a complex disorder with an impact on both the systemic and cellular levels. Oxidative stress seems to play a vital role in the pathomechanism of PXE but still needs to be further investigated. There has been evidence of systemic oxidative stress, supporting the metabolic hypothesis of PXE pathogenesis. Furthermore, investigations on patient-derived fibroblasts indicated oxidative stress on the cellular level as well, which provides evidence for the cellular hypothesis. Analyses on *ABCC6*-deficient human mesenchymal stem cells (hMSCs) regarding their oxidative status and senescence were performed to gain further insight into the cellular component of PXE pathogenesis.

A recent publication from Brampton et al. points to the bone marrow as a potential contributing factor in the PXE pathogenesis [10]. They were able to show that restoring the bone marrow of *Abbc6*-deficient mice with that of wildtype mice led to a significant reduction in the calcification of the whiskers and kidney. Interestingly, the transplantation of bone marrow from *Abcc6*-deficient mice into wildtype mice did not increase calcification [10]. Furthermore, Plümers et al. detected impairments in lipid trafficking, intra- and extracellular lipolysis, release of lipids and fatty acid neogenesis in adipocytes generated from *ABCC6*-deficient human mesenchymal stem cells (hMSCs) [25]. Due to these findings linking MSCs to the pathogenesis of PXE, hMSCs were chosen for this investigation. In accordance with Plümers et al., a CRISPR/Cas9-based approach for an *ABCC6* knockdown was chosen [25]. Due to the inability to generate single cell cultures, a cell pool containing homozygous, heterozygous and wildtype cells was used here and must be taken into account when interpreting the results of this study. Nevertheless, based on the results of this study regarding the CRISPR efficiency, the fraction of wildtype cells in the pool can be considered small. A knockdown efficiency of approximately 70% was confirmed using a T7 endonuclease I assay, TA-cloning and qRT-PCR. No mutations were detected in the three most common off-target gene regions, so off-target effects can be ruled out (Figure S2). However, it was not possible to confirm the knockdown at the protein level due to the lack of appropriate antibodies against human ABCC6 or ABCC6-specific activity assays. Given the sample size of n = 2, the results generated here were used solely to gain initial insights into the relationship between ABCC6 and oxidative stress in hMSCs. The consistency of the observed trends confirms the biological relevance of our results. Nevertheless, a larger sample size will be required for future studies in order to further confirm the observations made here.

The reactive oxygen species (ROS) and nitric oxide (NO) were investigated using fluorescent dyes to evaluate the oxidative status of knockdown cells in comparison to control cells. The incubation with $H_2O_2$ was chosen to mimic the systemic oxidative stress reported in PXE patients and the vitamin E derivate Trolox was used to counteract a potential increase in reactive species (RS) levels following *ABCC6* knockdown or $H_2O_2$ induction. The incubation with $H_2O_2$ increased the levels of total ROS and nitric oxide in both control and knockdown cells. This can be explained by the RS-inducing properties of $H_2O_2$ reported in the literature [26–28]. The additional treatment with Trolox reduced the levels of ROS and NO, emphasizing its antioxidative properties. After the knockdown of *ABCC6*, total ROS and NO were determined to be increased, possibly indicating oxidative stress in knockdown cells by induced production or reduced degradation of nitric oxide. Nitric oxide in mesenchymal stem cells is reported to have opposite effects depending on the concentration. While small concentrations were shown to promote cell survival and proliferation, higher concentrations can induce cell cycle arrest and senescence [29–31]. This suggests the hypothesis that the increased NO levels following the knockdown of *ABCC6* may induce a senescence-like phenotype. It should be noted that the fluorescent dyes used in this study may be influenced by experimental artefacts. The fluorescence of DCFDA may

be influenced by pH or metal ions, while it has been shown that DAF-FM may form fluorescent products through auto-oxidation or superoxide [32,33]. Therefore, the results shown here must be interpreted with caution. A higher β-galactosidase activity was detected for knockdown cells, indicating the presence of a senescence-like phenotype, therefore, the expression of NO synthetase could be investigated in future studies. Furthermore, the specific inhibition of NO formation by asymmetric dimethylarginine could give further insights into the possible association of NO levels and the senescence-like phenotype following *ABCC6* knockdown [34,35]. An indication of this connection was made by the incubation of knockdown cells with the antioxidant Trolox, resulting in decreased β-galactosidase activity and an attenuated senescence-like phenotype. This suggests that a decrease in oxidative stress in *ABCC6* knockdown cells may result in the reversal of the senescence-like phenotype detected. In addition, the β-galactosidase assay did not reveal any elevated activity for knockdown cells incubated with $H_2O_2$, indicating a possible resistance to additional oxidative stress. The senescence-like phenotype associated with PXE was also detected in patient-derived dermal fibroblasts, with elevated β-galactosidase activity in addition to increased secretion of interleukin 6 (IL-6) and a higher mRNA expression of *p21* but not *p53* [36]. In this study, an elevated mRNA expression of *p21* and *p53* was detected. The differences between this study and that of Tiemann et al. could be explained by the use of different cell types, since the senescence-associated secretory phenotype is highly cell-type specific [37]. The decrease in β-galactosidase activity by incubation with Trolox was not accompanied by a decreased mRNA expression of *p21* and *p53* in knockdown cells, which could be explained by post-transcriptional regulations influencing protein synthesis and activity. Immunofluorescence staining of p21 and p53 was performed to further investigate the influence of the cell cycle inhibitors on the senescence-like phenotype, revealing a strong increase in protein abundance for p53. In contrast to the β-galactosidase assay, the treatment of knockdown cells with $H_2O_2$ further increased the fluorescence signal of p53, while the additional treatment with Trolox counteracted this increase. It might be useful here to investigate the protein abundance and localization of phosphorylated p53 using immunofluorescence or a Western blot, since phosphorylated p53 is the transcriptionally active form [38,39]. The discrepancy between mRNA and protein expression observed for p21 indicates pronounced post-transcriptional regulation, which has already been demonstrated for *p21* [40].

The oxidative damage was evaluated using immunofluorescence staining with antibodies specific to 4-hydroxynonenal (4-HNE), a product of lipid peroxidation by oxidative stress [41]. It was shown that the knockdown of *ABCC6* resulted in increased lipid peroxidation, possibly due to the elevated ROS levels. Surprisingly, the incubation of cells with $H_2O_2$ did not result in any increased lipid peroxidation. This could be explained by the degradation of 4-HNE with time, which can be mediated by proteins such as aldose reductase, glutathione-S-transferases and aldehyde dehydrogenases. The expression or activity of these proteins could be investigated in future studies to better understand the absence of lipid peroxidation products in $H_2O_2$-treated control cells. The same procedure could also be applicable in knockdown cells incubated with $H_2O_2$, since they show no increase in lipid peroxidation either. Regarding the knockdown cells, the unaltered level of lipid peroxidation after $H_2O_2$ treatment could also be in accordance with the results of the β-galactosidase assay, showing no increased activity after treatment. Trolox was shown to decrease the level of 4-HNE fluorescence in knockdown cells, proving to be a suitable inhibitor of oxidative stress damage induced by ABCC6 deficiency. In contrast to this, the additional treatment with Trolox reduced the 4-HNE fluorescence signal only in control cells.

Sirtuins (SIRT) are a family of histone deacetylases with different functions in processes associated with oxidative stress defense [19,20]. The mRNA expression of *SIRT2*, *SIRT3*, *SIRT6* and *SIRT7* was shown to be upregulated by incubation with $H_2O_2$ in control cells and following *ABCC6* knockdown, while no change in mRNA expression was detectable in $H_2O_2$-treated knockdown cells. SIRT2 was shown to increase the expression of superoxide dismutase 1/2 and decrease oxidative stress and senescence through the inhibition of the p21/p53 pathway in nucleus pulposus cells [42]. In this study, mRNA expression of *SIRT2* could be a compensatory mechanism for the senescence-like phenotype following the $H_2O_2$ treatment of control cells and *ABCC6* knockdown. The sirtuins 3, 4 and 5 are localized in the mitochondria. Only the mRNA expression of *SIRT3* is altered by incubation with $H_2O_2$ or *ABCC6* knockdown; therefore, only a mildly, if any, altered mitochondrial oxidative stress can be assumed following $H_2O_2$-treatment and knockdown. Furthermore, SIRT3 was shown to deacetylate specific components of the electron transport chain to increase the oxidative phosphorylation and decrease its sensitivity to RS [43–45]. In addition, SIRT3 is an activator of fatty-acid oxidation in the mitochondria [46,47]. In accordance with the literature, these results suggest alterations in the mitochondrial energy metabolism and fatty-acid oxidation that require further investigation [7]. Knockout of SIRT6 promotes premature aging in mice [48]. It was shown that SIRT6 protects cells against oxidative stress-induced DNA damage and exerts highly cell type specific effects on proliferation [49–51]. Furthermore, a SIRT6 deficiency promotes the switch to anaerobic glycolysis, resulting in lactate generation and a decrease in mitochondrial oxidative phosphorylation [52]. In light of these reported functions of SIRT6, a compensatory upregulation due to the *ABCC6* knockdown and the increase in RS levels would be possible. In addition, the increased mRNA expression of *SIRT6* could be a sign of elevated aerobic glycolysis and ATP generation in mitochondria. This possibility has to be investigated in future studies. The function of SIRT7 is largely unknown, though it seems to regulate cell growth and metabolism, may be required for cell viability and modulates the stress response of cells to difficult circumstances [53–56]. A possible explanation for the upregulated mRNA expression of *SIRT7* would be the adaptation to the increased oxidative stress following *ABCC6* knockdown.

Regarding the mRNA expression of *GSS*, *GPX1* and *GPX4*, the same pattern of induced expression following $H_2O_2$ treatment and *ABCC6* knockdown with a lack of induction after the incubation of knockdown cells with $H_2O_2$ was detected. Glutathione is a very important cellular antioxidant protein that is synthesized by glutathione synthetase (GSS), whereby its antioxidant property is mostly mediated by glutathione peroxidases (GPX). Glutathione can be used to degrade $H_2O_2$ and lipid peroxides, generating glutathione disulfide that can be restored to maintain the cells' antioxidant defense [57]. The upregulation of mRNA expression detected could be a compensatory mechanism due to the induction of oxidative stress by incubation with $H_2O_2$ or *ABCC6* knockdown. Since no further elevation in mRNA expression was detectable after the $H_2O_2$ treatment of knockdown cells, the maximum induction may be reached due to the knockdown with no further elevation possible. The protective effects of increased *GSS* or *GPX1* mRNA expression against oxidative stress were shown in genetically engineered mice and chicken embryo fibroblasts [58,59]. The redox status of the knockdown hMSCs could be evaluated in further studies to investigate changes by the application of additional oxidative stress.

Regarding the mRNA expression of catalase (*CAT*), no changes were detected following *ABCC6* knockdown, indicating that the advanced oxidative defense of knockdown cells is based mainly on the glutathione system. The mRNA expression of TNF receptor associated protein 1 (*TRAP1*) was induced after the incubation of control cells with $H_2O_2$ and *ABCC6* knockdown. Since TRAP1 is a mitochondria-localized protein that protects against

oxidative stress, these results seem to contradict the lack of elevation of mitochondrial superoxide. However, there are different postulated functions of TRAP1 in the endoplasmic reticulum and the cytosol. TRAP1 seems to be a part of the tumor necrosis factor-α pathway and activates the transcription factor signal transducer and activator of transcription 3 (STAT3) [60]. In previous work, the JAK/STAT3 signaling pathway was shown to be activated in fibroblasts derived from PXE patients, resulting in increased inflammation [61]. The elevated expression of *TRAP1* may be one contributing factor of STAT3 activation.

## 5. Conclusions

The data obtained in this study suggest that knockdown of *ABCC6* leads to a p53-mediated senescence-like phenotype due to increased levels of reactive species. This is accompanied by increased lipid peroxidation and enhanced oxidative stress defenses, making knockdown cells insensitive to further oxidative stress. Some results point to defects in mitochondrial energy generation and fatty-acid oxidation that require further investigation. The antioxidant Trolox was shown to reduce reactive species levels in knockdown cells, leading to an attenuated senescence-like phenotype and lipid peroxidation but leaving the elevated oxidative stress defense unaltered. This study further emphasizes the impact of oxidative stress on the PXE phenotype and provides new indications for the use of antioxidants as a potential treatment for PXE.

**Supplementary Materials:** The following supporting information can be downloaded at https://www.mdpi.com/article/10.3390/antiox15020241/s1. Figure S1. Validation of CRISPR-Cas9 mediated ABCC6 knockdown. Figure S2. Sanger sequencing of possible off-targets. Figure S3. Mutational diversity in knockdown pools. Figure S4. Gating strategy of reactive species detection using flow cytometry. Table S1. Characteristics of the sequencing primers used in this study. Included are gene names, primer sequences, annealing temperatures and product sizes.

**Author Contributions:** Conceptualization, C.K. and D.H.; methodology, M.R.O.; validation, M.R.O.; formal analysis, M.R.O.; investigation, M.R.O.; resources, C.K. and D.H.; data curation, M.R.O.; writing—original draft preparation, M.R.O.; writing—review and editing, C.K. and D.H.; visualization, M.R.O.; supervision, C.K.; project administration, D.H. All authors have read and agreed to the published version of the manuscript.

**Funding:** Publication was funded by Open Access (OA) Fund of the Ruhr-Universität Bochum.

**Institutional Review Board Statement:** Ethical review and approval were waived for this study due to the use of commercial human cell lines.

**Informed Consent Statement:** Patient consent was waived due to the use of commercial human cell lines.

**Data Availability Statement:** The original raw data and materials presented in the study will be made available upon request. Further inquiries can be directed to the corresponding author.

**Acknowledgments:** We thank Philip Saunders for his linguistic advice.

**Conflicts of Interest:** The authors declare no conflicts of interest.

## Abbreviations

The following abbreviations are used in this manuscript:

| | |
|---|---|
| ·O2- | Superoxide |
| 4-HNE | 4-Hydroxynonenal |
| ABCC6 | ATP binding cassette subfamily C member 6 |
| ANOVA | Analysis of variance |
| ATP | Adenosine triphosphate |
| CAT | Catalase |

| | |
|---|---|
| CRISPR | Clustered regularly interspaced short palindromic repeat |
| crRNA | CRISPR RNA |
| DAF-FM | 4-Amino-5-methylamino-2′,7′-difluorofluorescein diacetate |
| DCFCA | 6-Carboxy-2′,7′-dichlordihydrofluorescein-diacetat |
| GPX | Glutathione peroxidase |
| GSS | Glutathione synthetase |
| $H_2O_2$ | Hydrogen peroxide |
| hMSCs | Human mesenchymal stem cells |
| IL | Interleukin |
| JAK | Janus kinase |
| NO | Nitric oxide |
| PXE | Pseudoxanthoma elasticum |
| qRT-PCR | Quantitative real time polymerase chain reaction |
| ROS | Reactive oxygen species |
| RS | Reactive species |
| SEM | Standard error of mean |
| SIRT | Sirtuin |
| STAT | Signal transducer and activator of transcription |
| TRAP1 | Tumor necrosis factor receptor associated protein 1 |

## References


1. Le Saux, O.; Martin, L.; Aherrahrou, Z.; Leftheriotis, G.; Váradi, A.; Brampton, C.N. The molecular and physiological roles of ABCC6: More than meets the eye. *Front. Genet.* **2012**, *3*, 289. [CrossRef]
2. Bergen, A.A.B.; Plomp, A.S.; Schuurman, E.J.; Terry, S.; Breuning, M.; Dauwerse, H.; Swart, J.; Kool, M.; van Soest, S.; Baas, F.; et al. Mutations in ABCC6 cause *Pseudoxanthoma elasticum*. *Nat. Genet.* **2000**, *25*, 228–231. [CrossRef]
3. Madon, J.; Hagenbuch, B.; Landmann, L.; Meier, P.J.; Stieger, B. Transport function and hepatocellular localization of mrp6 in rat liver. *Mol. Pharmacol.* **2000**, *57*, 634–641. [CrossRef]
4. Beck, K.; Hayashi, K.; Nishiguchi, B.; Le Saux, O.; Hayashi, M.; Boyd, D.B. The distribution of Abcc6 in normal mouse tissues suggests multiple functions for this ABC transporter. *J. Histochem. Cytochem.* **2003**, *51*, 887–902. [CrossRef]
5. Moitra, K.; Garcia, S.; Jaldin, M.; Etoundi, C.; Cooper, D.; Roland, A.; Dixon, P.; Reyes, S.; Turan, S.; Terry, S.; et al. ABCC6 and *Pseudoxanthoma elasticum*: The face of a rare disease from genetics to advocacy. *Int. J. Mol. Sci.* **2017**, *18*, 1488. [CrossRef] [PubMed]
6. Li, Q.; Jiang, Q.; Pfendner, E.; Váradi, A.; Uitto, J. *Pseudoxanthoma elasticum*: Clinical phenotypes, molecular genetics and putative pathomechanisms. *Exp. Dermatol.* **2009**, *18*, 1–11. [CrossRef]
7. Lofaro, F.D.; Boraldi, F.; Garcia-Fernandez, M.; Estrella, L.; Valdivieslo, P.; Quaglino, D. Relationship between mitochondrial structure and bioenergetics in *Pseudoxanthoma elasticum* dermal fibroblasts. *Front. Cell Dev. Biol.* **2020**, *8*, 610266. [CrossRef]
8. Pasquali-Ronchetti, I.; Garcia-Fernandez, M.; Boraldi, F.; Quaglino, D.; Gheduzzi, D.; De Vincenzi Paolinelli, C.; Tiozzo, R.; Bergamini, S.; Ceccarelli, D.; Muscatello, U. Oxidative stress in fibroblasts from patients with *Pseudoxanthoma elasticum*: Possible role in the pathogenesis of clinical manifestations. *J. Pathol.* **2006**, *208*, 54–61. [CrossRef]
9. Garcia-Fernandez, M.I.; Gheduzi, D.; Boraldi, F.; Devincenzi Paolinelli, C.; Sanchez, P.; Valdovielso, P.; Morilla, M.J.; Quaglino, D.; Guerra, D.; Casolari, S.; et al. Parameters of oxidative stress are present in the circulation of PXE patients. *Biochim. Biophys. Acta BBA-Mol. Basis Dis.* **2008**, *1782*, 474–481. [CrossRef] [PubMed]
10. Takai, H.; Smogorzewska, A.; De Lange, T. DNA damage foci at dysfunctional telomeres. *Curr. Biol.* **2003**, *13*, 1549–1556. [CrossRef] [PubMed]
11. Zhang, L.; Pitcher, L.E.; Yousefzadeh, M.J.; Niederhofer, L.J.; Robbins, P.D.; Zhu, Y. Cellular senescence: A key therapeutic target in aging and diseases. *J. Clin. Investig.* **2022**, *132*, e158450. [CrossRef]
12. Rodier, F.; Campisi, J. Four faces of cellular senescence. *J. Cell Biol.* **2022**, *192*, 547–556. [CrossRef]
13. Lee, A.C.; Fenster, B.E.; Ito, H.; Takeda, K.; Bae, N.S.; Hirai, T.; Yu, Z.-X.; Ferrans, V.J.; Howard, B.N.; Finkel, T. Ras Proteins induce senescence by altering the intracellular levels of reactive oxygen species. *J. Biol. Chem.* **1999**, *274*, 7936–7940. [CrossRef]
14. Passos, J.F.; Nelson, G.; Wang, C.; Richter, T.; Simillion, C.; Proctor, C.J.; Miwa, S.; Olijslagers, S.; Hallinan, J.; Wipat, A.; et al. Feedback between p21 and reactive oxygen production is necessary for cell senescence. *Mol. Syst. Biol.* **2010**, *6*, MSB20105. [CrossRef]
15. Park, J.-H.; Kim, T.-Y.; Jong, H.-S.; Kim, T.Y.; Chun, Y.-S.; Park, J.-W.; Lee, C.-T.; Jung, H.C.; Kim, N.K.; Bang, Y.-J. Gastric epithelial reactive oxygen species prevent normoxic degradation of hypoxia-inducible factor-1 in gastric cancer cells. *Clin. Cancer Res.* **2003**, *9*, 433–440.

16. Meyer, M.; Schreck, R.; Baeuerle, P.A. H202 and antioxidants have opposite effects on activation of NF-xB and AP-1 in intact cells: AP-1 as secondary antioxidant-responsive factor. *EMBO J.* **1993**, *12*, 2005–2015. [CrossRef] [PubMed]
17. Simon, A.R.; Rai, U.; Fanburg, B.L.; Cochran, B.H. Activation of the JAK-STAT pathway by reactive oxygen species. *Am. J. Physiol.-Cell Physiol.* **1998**, *275*, C1640–C1652. [CrossRef] [PubMed]
18. Davalli, P.; Mitic, T.; Caporali, A.; Lauriola, A.; D'Arca, D. ROS, cell senescence, and novel molecular mechanisms in aging and age-related diseases. *Oxidative Med. Cell. Longev.* **2016**, *2016*, 3565127. [CrossRef]
19. Singh, C.K.; Chhabra, G.; Ndiaye, M.A.; Garcia-Peterson, L.M.; Mack, N.J.; Ahmad, N. The role of sirtuins in antioxidant and redox signaling. *Antioxid. Redox Signal.* **2018**, *28*, 643–661. [CrossRef]
20. Imai, S.; Armstrong, C.M.; Kaeberlein, M.; Guarente, L. Transcriptional silencing and longevity protein Sir2 is an NAD-dependent histone deacetylase. *Nature* **2000**, *403*, 795–800. [CrossRef]
21. Standing, A.S.; Hong, Y.; Paisan-Ruiz, C.; Omoyinmi, E.; Medlar, A.; Stanescu, H.; Kleta, R.; Rowcenzio, D.; Hawkins, P.; Lachmann, H.; et al. TRAP1 chaperone protein mutations and autoinflammation. *Life Sci. Alliance* **2020**, *3*, e201900376. [CrossRef]
22. Kuilman, T.; Nichaloglou, C.; Vredeveld, L.C.W.; Douma, S.; van Doorn, R.; Desmet, C.J.; Arden, L.A.; Mooi, W.J.; Peeper, D.S. Oncogene-induced senescence relayed by an interleukin-dependent inflammatory network. *Cell* **2008**, *133*, 1019–1031. [CrossRef]
23. Lee, B.Y.; Han, J.A.; Im, J.S.; Morrone, A.; Johung, K.; Goodwin, E.C.; Kleijer, W.J.; DiMaio, D.; Hwang, E.S. Senescence-associated β-galactosidase is lysosomal β-galactosidase. *Aging Cell* **2006**, *5*, 187–195. [CrossRef]
24. Brampton, C.; Pomozi, V.; Le Corre, Y.; Zoll, J.; Kauffenstein, G.; Ma, C.; Hoffman, P.R.; Martin, L.; Le Saux, O. Bone marrow–derived ABCC6 is an essential regulator of ectopic calcification in *Pseudoxanthoma elasticum*. *J. Investig. Dermatol.* **2024**, *144*, 1772–1783.e3. [CrossRef] [PubMed]
25. Plümers, R.; Osterhage, M.R.; Lindenkamp, C.; Knabbe, C.; Hendig, D. Targeting ABCC6 in mesenchymal stem cells: Impairment of mature adipocyte lipid homeostasis. *Int. J. Mol. Sci.* **2022**, *23*, 9218. [CrossRef]
26. Gary, R.K.; Kindell, S.M. Quantitative assay of senescence-associated β-galactosidase activity in mammalian cell extracts. *Anal. Biochem.* **2005**, *343*, 329–334. [CrossRef] [PubMed]
27. Dávila, D.; Torres-Aleman, I. Neuronal death by oxidative stress involves activation of $FOXO_3$ through a two-arm pathway that activates stress kinases and attenuates insulin-like growth factor I signaling. *Mol. Biol. Cell* **2008**, *19*, 2014–2025. [CrossRef]
28. Chen, L.; Liu, L.; Yin, J.; Luo, Y.; Huang, S. Hydrogen peroxide-induced neuronal apoptosis is associated with inhibition of protein phosphatase 2A and 5, leading to activation of MAPK pathway. *Int. J. Biochem. Cell Biol.* **2009**, *41*, 1284–1295. [CrossRef] [PubMed]
29. Ugusman, A.; Zakaria, Z.; Hui, C.K.; Nordin, N.A.M.M. Piper sarmentosum increases nitric oxide production in oxidative stress: A study on human umbilical vein endothelial cells. *Clinics* **2010**, *65*, 709–714. [CrossRef]
30. Van de Wouwer, M.; Couzinié, C.; Serrano-Palero, M.; González-Fernández, Ó.; Galmés-Varela, C.; Menéndez-Antolí, P.; Grau, L.; Villalobo, A. Activation of the BRCA1/Chk1/p53/p21Cip1/Waf1 pathway by nitric oxide and cell cycle arrest in human neuroblastoma NB69 cells. *Nitric Oxide* **2012**, *26*, 182–191. [CrossRef]
31. Bonafè, F.; Guarnieri, C.; Muscari, C. Nitric oxide regulates multiple functions and fate of adult progenitor and stem cells. *J. Physiol. Biochem.* **2015**, *71*, 141–153. [CrossRef]
32. Thomas, D.D.; Ridnour, L.A.; Isenberg, J.S.; Flores-Santana, W.; Switzer, C.H.; Donzelli, S.; Hussain, P.; Vecoli, C.; Paolocci, N.; Ambs, A.; et al. The chemical biology of nitric oxide: Implications in cellular signaling. *Free Radic. Biol. Med.* **2008**, *45*, 18–31. [CrossRef]
33. Balcerczyk, A.; Soszynski, M.; Bartosz, G. On the specificity of 4-amino-5-methylamino-2′,7′-difluorofluorescein as a probe for nitric oxide. *Free Radic. Biol. Med.* **2005**, *39*, 327–335. [CrossRef] [PubMed]
34. Murphy, M.P.; Bayir, H.; Belousov, V.; Chang, C.J.; Davies, K.J.A.; Davies, M.J.; Dick, T.P.; Finkel, T.; Forman, H.J.; Janssen-Heiningeret, Y.; et al. Guidelines for measuring reactive oxygen species and oxidative damage in cells and in vivo. *Nat. Metab.* **2022**, *4*, 651–662. [CrossRef] [PubMed]
35. MacAllister, R.J.; Whitley, G.S.J.; Vallance, P. Effects of guanidino and uremic compounds on nitric oxide pathways. *Kidney Int.* **1994**, *45*, 737–742. [CrossRef] [PubMed]
36. Leone, A.; Moncada, S.; Vallance, P.; Calver, A.; Collier, J. Accumulation of an endogenous inhibitor of nitric oxide syn-thesis in chronic renal failure. *Lancet* **1992**, *339*, 572–575. [CrossRef]
37. Tiemann, J.; Wagner, T.; Lindenkamp, C.; Plümers, R.; Faust, I.; Knabbe, C.; Hendig, D. Linking ABCC6 deficiency in primary human dermal fibroblasts of PXE patients to p21-mediated premature cellular senescence and the development of a proinflammatory secretory phenotype. *Int. J. Mol. Sci.* **2020**, *21*, 9665. [CrossRef]
38. Głuchowska, A.; Cysewski, D.; Baj-Krzsworzeka, M.; Szatanek, R.; Węglarczyk, K.; Podszywałow-Bartnicka, P.; Sunderland, P.; Kozłowska, E.; Śliwińska, M.A.; Dąbrowski, M.; et al. Unbiased proteomic analysis of extracellular vesicles secreted by senescent human vascular smooth muscle cells reveals their ability to modulate immune cell functions. *GeroScience* **2022**, *44*, 2863–2884. [CrossRef]
39. Dumaz, N.; Meek, D.W. Serine15 phosphorylation stimulates p53 transactivation but does not directly influence interaction with HDM2. *EMBO J.* **1999**, *18*, 7002–7010. [CrossRef]

40. Jung, Y.-S.; Qian, Y.; Chen, X. Examination of the expanding pathways for the regulation of p21 expression and activity. *Cell Signal.* **2010**, *22*, 1003–1012. [CrossRef]
41. Uchida, K. 4-Hydroxy-2-nonenal: A product and mediator of oxidative stress. *Prog. Lipid Res.* **2003**, *42*, 318–343. [CrossRef]
42. Yang, M.; Peng, Y.; Liu, W.; Zhou, M.; Meng, Q.; Yuan, C. Sirtuin 2 expression suppresses oxidative stress and senescence of nucleus pulposus cells through inhibition of the p53/p21 pathway. *Biochem. Biophys. Res. Commun.* **2019**, *513*, 616–622. [CrossRef]
43. Ahn, B.-H.; Kim, H.-S.; Song, S.; Lee, I.-H.; Vassilopoulos, A.; Deng, C.-X.; Finkel, T. A role for the mitochondrial deacetylase Sirt3 in regulating energy homeostasis. *Proc. Natl. Acad. Sci. USA* **2008**, *105*, 14447–14452. [CrossRef]
44. Lombard, D.B.; Alt, F.W.; Cheng, H.-L.; Bunkenborg, J.; Streeper, R.S.; Mostoslavsky, R.; Kim, J.; Yancopoulos, G.; Valenzuela, D.; Murphy, A.; et al. Mammalian Sir2 homolog SIRT3 regulates global mitochondrial lysine acetylation. *Mol. Cell. Biol.* **2007**, *27*, 8807–8814. [CrossRef] [PubMed]
45. Someya, S.; Yu, W.; Hallows, W.C.; Xu, J.; Vann, J.M.; Leeuwenburgh, C.; Tanokura, M.; Denu, J.M.; Prolla, T.A. Sirt3 mediates reduction of oxidative damage and prevention of age-related hearing loss under caloric restriction. *Cell* **2010**, *143*, 802–812. [CrossRef] [PubMed]
46. Hallows, W.C.; Yu, W.; Smith, B.C.; Devires, M.K.; Ellinger, J.J.; Someya, S.; Shortreed, M.R.; Prolla, T.; Markley, J.L.; Smith, L.M.; et al. Sirt3 promotes the urea cycle and fatty acid oxidation during dietary restriction. *Mol. Cell* **2011**, *41*, 139–149. [CrossRef]
47. Hirschey, M.D.; Shimazu, T.; Goetzman, E.; Jing, E.; Schwer, B.; Lombard, D.B.; Grueter, C.A.; Harris, C.; Biddinger, S.; Ilkayeva, O.R.; et al. SIRT3 regulates fatty acid oxidation via reversible enzyme deacetylation. *Nature* **2010**, *464*, 121–125. [CrossRef] [PubMed]
48. Mostoslavsky, R.; Chua, K.F.; Lombard, D.B.; Pang, W.W.; Fischer, M.R.; Gellon, L.; Liu, P.; Mostoslavsky, G.; Franco, S.; Murphy, M.M.; et al. Genomic instability and aging-like phenotype in the absence of mammalian SIRT6. *Cell* **2006**, *124*, 315–329. [CrossRef]
49. Pan, H.; Guan, D.; Liu, X.; Li, J.; Wang, L.; Wu, J.; Zhou, J.; Zhang, W.; Ren, R.; Zhang, W.; et al. SIRT6 safeguards human mesenchymal stem cells from oxidative stress by coactivating NRF2. *Cell Res.* **2016**, *26*, 190–205. [CrossRef]
50. Mao, Z.; Hine, C.; Tian, X.; Van Meter, M.; Au, M.; Vaidya, A.; Seluanov, A.; Gorbunova, V. SIRT6 promotes DNA repair under stress by activating PARP1. *Science* **2011**, *332*, 1443–1446. [CrossRef]
51. Van Meter, M.; Mao, Z.; Gorbunova, V.; Seluanov, A. SIRT6 overexpression induces massive apoptosis in cancer cells but not in normal cells. *Cell Cycle* **2011**, *10*, 3153–3158. [CrossRef]
52. Zhong, L.; Mostoslavsky, R. SIRT6 A master epigenetic gatekeeper of glucose metabolism. *Transcription* **2010**, *1*, 17–21. [CrossRef]
53. Ford, E.; Voit, R.; Liszt, G.; Magin, C.; Grummt, I.; Guarente, L. Mammalian Sir2 homolog SIRT7 is an activator of RNA polymerase I transcription. *Genes Dev.* **2006**, *20*, 1075–1080. [CrossRef] [PubMed]
54. Haigis, M.C.; Guarente, L.P. Mammalian sirtuins—Emerging roles in physiology, aging, and calorie restriction. *Genes Dev.* **2006**, *20*, 2913–2921. [CrossRef] [PubMed]
55. Shin, J.; He, M.; Liu, Y.; Paredes, S.; Villanova, L.; Brown, K.; Qiu, X.; Nabavi, N.; Mohrin, M.; Wojnoonski, K.; et al. SIRT7 represses myc activity to suppress ER stress and prevent fatty liver disease. *Cell Rep.* **2013**, *5*, 654–665. [CrossRef] [PubMed]
56. Chen, H.; Yang, Z.; Sun, Y.; Yin, S.; Tang, M.; Zhang, F. Targeting the key enzymes of abnormal fatty acid β-oxidation as a potential strategy for tumor therapy. *Front. Biosci.* **2022**, *27*, 95. [CrossRef]
57. Lu, S.C. Regulation of glutathione synthesis. *Mol. Asp. Med.* **2009**, *30*, 42–59. [CrossRef]
58. Yun, J.-W.; Lum, K.; Lei, X.G. A novel up-regulation of glutathione peroxidase 1 by knockout of liver regenerating protein Reg3β aggravates acetaminophen-induced hepatic protein nitration. *Free Radic. Biol. Med.* **2013**, *65*, 291–300. [CrossRef]
59. Lin, J.; Min, R.; Yi, X.; Zhuang, Y. Overexpression of glutathione synthetase gene improving redox homeostasis and chicken infectious bursal disease virus propagation in chicken embryo fibroblast DF-1. *Bioresour. Bioprocess.* **2023**, *10*, 60. [CrossRef]
60. Ramos Rego, I.; Santos Cruz, B.; Ambrósio, A.F.; Alves, C.H. TRAP1 in oxidative stress and neurodegeneration. *Antioxidants* **2021**, *10*, 1829. [CrossRef]
61. Lindenkamp, C.; Plümers, R.; Osterhage, M.R.; Vanakker, O.M.; Van Wynsberghe, J.; Knabbe, C.; Hendig, D. The activation of JAK/STAT3 signaling and the complement system modulate inflammation in the primary human dermal fibroblasts of PXE patients. *Biomedicines* **2023**, *11*, 2673. [CrossRef] [PubMed]


**Disclaimer/Publisher's Note:** The statements, opinions and data contained in all publications are solely those of the individual author(s) and contributor(s) and not of MDPI and/or the editor(s). MDPI and/or the editor(s) disclaim responsibility for any injury to people or property resulting from any ideas, methods, instructions or products referred to in the content.